



Published in final edited form as:

Comput Cardiol. 2009 January 1; 36: 49–52.

Dynamic Cardiovagal Response to Motion Sickness: A Point-Process Heart Rate Variability Study

LT LaCount³, V Napadow^{3,4}, B Kuo⁵, K Park^{3,6}, J Kim^{3,6}, EN Brown^{1,2}, and R Barbieri^{1,2}

¹Department of Anesthesia and Critical Care, Massachusetts General Hospital, Boston, MA, USA

²Dept of Brain and Cognitive Science, Massachusetts Institute of Technology, Cambridge, MA, USA

³MGH/MIT/HMS Martinos Center for Biomedical Imaging, Dept of Radiology, MGH, Charlestown, MA, USA

⁴Dept of Radiology, Logan College of Chiropractic, Chesterfield, MO, USA

⁵Gastroenterology Unit, MGH, Harvard Medical School, Boston, MA, USA

⁶Dept of Biomedical Engineering, Kyunghee University, Yongin, Republic of Korea

Abstract

A visual display of stripes was used to examine cardio-vagal response to motion sickness. Heart rate variability (HRV) was investigated using dynamic methods to discern instantaneous fluctuations in reaction to stimulus and perception-based events. A novel point process adaptive recursive algorithm was applied to the R-R series to compute instantaneous heart rate, HRV, and high frequency (HF) power as a marker of vagal activity. Results show interesting dynamic trends in each of the considered subjects. HF power averaged across ten subjects indicates a significant decrease 20s to 60s following the transition from “no nausea” to “mild.” Conversely, right before “strong” nausea, the group average shows a transient trending increase in HF power. Findings confirm gradual sympathetic activation with increasing nausea, and further evidence transitory increases in vagal tone before flushes of strong nausea.

1. Introduction

Nausea is a commonly occurring symptom typified by epigastric discomfort with the urge to vomit. It can arise from a variety of causes including as a side effect of pharmacotherapy and general anesthesia. Nausea has also been associated with pregnancy, and is seen with visual/vestibular sensory discordance. This latter cause, termed motion sickness, has been commonly adopted in experimental settings to study physiological response during nausea [1]. Individual symptoms of motion sickness can be dissociated along different axes using factor analysis [2]. These factors include nausea (e.g. stomach awareness, burping, increased salivation, sweating, and nausea), oculomotor (e.g. eye strain, difficulty focusing, blurred vision, headache), and disorientation (dizziness, vertigo).

Most previous motion sickness studies have involved the application of a nauseagenic stimulus or sequence of stimuli for a predetermined amount of time which may be terminated by the subject at any time [3-6]. In some studies the stimulus was interrupted or partially interrupted to ask subjects to subjectively score their nausea symptoms [3,6,7], while in others subjects

were asked after the completion of the experiment [8] or during the experiment without interrupting the stimulus [9,10]. Prior studies have investigated the response of the high frequency portion of heart rate variability, a measure of vagal activity, to motion sickness [11]. Measurement techniques used to find the response of heart rate variability to motion sickness have varied and the findings have been inconsistent [8,9].

In this study, a visual display of stripes was used to study the response of the autonomic nervous system to motion sickness. Heart rate variability, specifically the high frequency range, was studied using dynamic methods to discern instantaneous fluctuations in reaction to stimulus-based or perception-based events.

2. Methods

Protocol

19 female subjects with a mean age of 29.1 (s.d.=8.7) and a history of motion sickness symptoms as indicated by a score of greater than 60 on the Motion Sickness Susceptibility Questionnaire [12] participated in this study. Informed consent was obtained from all participants, and the protocol was approved by the Human Research Committee of Massachusetts General Hospital. The procedure was divided into three different periods. The first and last periods were each five minutes in length, during which subjects were asked to lie still and stare directly ahead at a cross-hair projected onto the center of a screen which took up the entire field of view (150°) of the subject. Between these two resting periods subjects were presented with a visual stimulus of stripes (black stripes 1.2cm, 6.9° viewing angle; white stripes 1.85cm, 10.6° viewing angle) translating left-to-right at an apparent speed of $62.5^\circ/\text{sec}$. The maximum stimulus time was 20 minutes, shortened in some subjects based on the individual subject's level of discomfort. In this session, during and after the nausea stimulus subjects used a button box to rate their overall nausea level ranging from "0" to "4", with a rating of "4" indicating "severe", a rating of "3" indicating "strong", a rating of "2" indicating "moderate", a rating of "1" indicating "mild", and a rating of "0" indicating no nausea. Subjects remained lying supine during the entire procedure.

Recordings

The electrocardiogram (ECG) signal was collected with an MRI-compatible Patient Monitor (Model 3150, InVivo Research, Inc., Orlando, FL) through MRI-compatible electrodes (VerMed, Bellows Falls, VT) on the chest. During the experiment, skin conductance level and respiration were also measured. All physiological signals were collected at 400 Hz using Chart Data Acquisition Software on a laptop using a 16 Channel Powerlab System (ADInstruments, Colorado Springs, CO). Respiration and fMRI data are detailed in another publication.

Signal Processing Analysis

A novel adaptive recursive algorithm was applied to the R–R series to compute instantaneous estimates of heart rate and heart rate variability from electrocardiogram recordings of R-wave events. This approach is based on the point process methods already used to develop both local likelihood [14] and adaptive [15] heart rate estimation algorithms. This novel assessment of heart rate variability has been also applied successfully in conjunction with fMRI recordings to characterize brain correlates of autonomic modulation [16]. The stochastic structure in the R–R intervals is modeled as an inverse Gaussian renewal process. The inverse Gaussian probability density is derived directly from an elementary, physiologically-based integrate-and-fire model [14,15]. The model also represents the dependence of the R–R interval length on the recent history of parasympathetic and sympathetic inputs to the SA node by modeling the mean as a linear function of the last p R–R intervals. This set of p coefficients allows for estimation of the spectral power (HRV) and further decomposition into classic low frequency

(LF, 0.04-0.15 Hz) and high frequency (HF, 0.15-0.5 Hz) spectral components. The point process recursive algorithm is able to estimate the dynamics of the model parameters, and consequently the time-varying behavior of each spectral index, at any time resolution. This statistical model for deriving the HRV timeseries has been cross-validated with standard time-frequency domain approaches for HRV analysis [14]. The dynamic response for the point process method was found to provide a significant improvement in tracking fast dynamic changes when compared to the more conventional RLS algorithm [15]. A fixed order $p=8$ was chosen for the analysis. Indices were updated every 10 ms and then resampled at 2 Hz. Raw R-R interval, instantaneous heart rate, instantaneous heart rate variability, and point-process HF are shown for an individual subject along with that subject's nausea ratings in Figure 1.

Statistical Analysis

Point-process HF data were analyzed by comparing points between 30 seconds before a point of interest (the onset of the nausea stimulus, "START"; increase to a rating level of "1", "0-1"; increase to a rating level of "2", "1-2"; increase to a rating level of "3", "2-3"; termination of nausea stimulus, "END") to 60 seconds after that point of interest. This region was chosen to reveal responses of HF to a specific event occurring on a short time scale. Each averaged second of time beginning 20 seconds before the given point of interest through 60 seconds following that point of interest was compared to the average of the region between 30 to 20 seconds before the point of interest using a t-test paired across subjects (Matlab v. 7.1, The MathWorks, Inc., Natick, MA). A p-value of less than 0.05 was considered significantly different from the baseline region for that point, while a p-value between 0.1 and 0.05 was considered a trending increase or decrease over baseline level.

3. Results

Of 19 subjects who completed the experiment, seven were not included in our analyses because their maximum nausea rating was below a "4," and one was not included because her baseline nausea level rating was a "2," while all other subjects began at "0." Heart rate and R-R interval could not be determined from one subject's ECG data, and therefore that subject was also excluded.

Figure 1 shows the resulting instantaneous HR, HRV and HF power time series estimated for one subject. This example shows very interesting dynamics. Focusing on the HF power as compared to SCL, note the sharp vagal activation at 430s (increase in HF power) immediately before the subject reports mild nausea, followed by a sympathetic burst (SCL increases at around 460 s). Also note a similar phenomenon at 720s. Here, HF begins to increase from minimum levels to a peak before the subject reports increasing nausea to level "3" at around 740s, followed by a sympathetic burst (SCL increases at around 750 s). During level "3" SCL seems to stabilize at higher sympathetic levels, while a low vagal background tone is interrupted by long transient increases centered around 950 s and 1200 s. After the second transient, higher sympathetic activity is observed until the subjects report severe nausea. The general slow trends observed in the single subject are reflected in the stationary statistical averages across subject (Table 1). Here we observe a gradual, significant increase in HR and SCL, and a parallel increase in HF with increasing nausea.

In the dynamic statistical analysis, the point-process HF power estimates were selected during five 90 second regions of interest: onset of the nausea stimulus, "START"; increase to a rating level of "1," "0-1"; increase to a rating level of "2," "1-2"; increase to a rating level of "3," "2-3"; and termination of nausea stimulus, "END". An average over all subjects within highlighted ("+" for $0.1 > p > 0.05$; "*" for $p < 0.05$) is shown in Figure 2. As the stimulus starts, HF begins to decrease (Fig. 2B) and keeps a decreasing trend all along the experiment. The "0-1" panel (Fig. 2C) shows a region of statistically significant decrease from the baseline level

a few seconds following the rating increase to “1”. Importantly, the decreasing trend is interrupted by sharp peaks (despite the average), at around 15-20 s before the rating increase to “2” and “3” (D and E respectively), significant in the second case, and a smoother increasing bump also appears before the increase to “4” (F).

4. Discussion and conclusions

This experiment employed a visual stimulus of translating stripes to induce motion sickness in supine subjects, while measuring heart rate variability in relation to the stimulus and each subject's perception of sickness level. We have presented here a novel dynamic approach to analyzing heart rate variability in relation to nausea. Previous studies [5,8,9] have examined the effect of motion sickness-induced nausea on measures of heart rate variability, but the findings have been variable.

The high frequency range of heart rate variability is considered to be representative of vagal activity. Previous studies have shown a decrease in HF between rest and nauseogenic stimulus [8] or an increase in HF between rest and stimulus [9]. However, in both other studies subjects were seated [8,9], and in one study the subject was also rotating [8], whereas in our study subjects remained stationary and lying supine.

We utilized a dynamic point process approach to measure HF variations (as well as instantaneous indices of HR and HRV) at a millisecond timescale. Stationary statistical analysis confirms a gradual prevailing sympathetic drive, as reflected by significantly increasing values of SCL and HR across stronger nausea levels, accompanied by a parallel decrease in vagal tone as measured by the HF power index. Dynamic results also reveal gradual decreases in HF power in response to increases in nausea levels and further show important transient increases before the transitions, particularly significant for the group before the rating of “3”. This means that our dynamic estimates are able to discern short term fluctuations in high frequency heart rate variability response to specific events with respect to a baseline a few seconds before a given event, as well as following the event.

In summary, our results indicate that, while the initial rating increase to mild nausea results in a significant decrease in vagal activity, HF power dynamic fluctuations indicate short term autonomic bursts before rating increases to stronger nausea levels. As stationary findings confirm a general sympathetic activation with increasing nausea, the instantaneous estimates provide a novel, high-resolution dynamic characterization capable of discerning transitory increases in vagal tone right before the subject reports flushes of strong nausea.

Acknowledgments

We would like to thank NIH for funding support (RB: R01-HL084502; EB: R01-DA015644 and DP1-OD003646; VN: K01-AT002166, P01-AT002048; KP: F05-AT003770; BK: K23-DK069614), the National Center for Complementary and Alternative Medicine (P41RR14075; CRC 1 UL1 RR025758-01), the Mental Illness and Neuroscience Discovery (MIND) Institute, and the International Foundation of Functional GI Disorders. Dr. Park was also supported by the Institute of Information Technology Advancement, Korea IITA-2008-(C1090-0801-0002).

References

1. Koch KL. Illusory self-motion and motion sickness: a model for brain-gut interactions and nausea. *Dig Dis Sci* 1999;44:53S–57S. [PubMed: 10490040]
2. Kennedy RS, Berbaum KS, Lilienthal MG, Smith MG. Disorientation and natural disequilibrium from simulated flight. *International Symposium on Aviation Psychology* 1993;7:799–804.
3. Cowings PS, Suter S, Toscano WB, Kamiya J, Naifeh K. General autonomic components of motion sickness. *Psychophysiology* 1986;23:542–51. [PubMed: 3809361]

4. Isu N, Koo J, Takahashi N. Changes of skin potential level and of skin resistance level corresponding to lasting motion discomfort. *Aviat Space Environ Med* 1987;58:136–42. [PubMed: 3827789]
5. Mullen TJ, Berger RD, Oman CM, Cohen RJ. Human heart rate variability relation is unchanged during motion sickness. *J Vestib Res* 1998;8:95–105. [PubMed: 9416595]
6. Stout CS, Toscano WB, Cowings PS. Reliability of psychophysiological responses across multiple motion sickness stimulation tests. *J Vestib Res* 1995;5:25–33. [PubMed: 7711945]
7. Graybiel A, Lackner JR. Evaluation of the relationship between motion sickness symptomatology and blood pressure, heart rate, and body temperature. *Aviat Space Environ Med* 1980;51:211–4. [PubMed: 7362567]
8. Doweck I, Gordon CR, Shlitner A, Spitzer O, Gonen A, Binah O, elamed M, Shupak A. Alterations in R-R variability associated with experimental motion sickness. *J Auton Nerv Syst* 1997;67:31–7. [PubMed: 9470142]
9. Kim YY, Kim HJ, Kim EN, Ko HD, Kim HT. Characteristic changes in the physiological components of cybersickness. *Psychophysiology* 2005;42:616–25. [PubMed: 16176385]
10. Miller JC, Sharkey TJ, Graham GA, McCauley ME. Autonomic physiological data associated with simulator discomfort. *Aviat Space Environ Med* 1993;64:813–9. [PubMed: 8216142]
11. Heart rate variability. Standards of measurement, physiological interpretation, and clinical use. Task Force of the European Society of Cardiology and the North American Society of Pacing and Electrophysiology. *Eur Heart J* 1996;17:354–81. [PubMed: 8737210]
12. Golding JF. Motion sickness susceptibility questionnaire revised and its relationship to other forms of sickness. *Brain Res Bull* 1998;47:507–16. [PubMed: 10052582]
13. Goldberger AL, Amaral LA, Glass L, Hausdorff JM, Ivanov PC, Mark RG, Mietus JE, Moody GB, Peng CK, Stanley HE. PhysioBank, PhysioToolkit, and PhysioNet: components of a new research resource for complex physiologic signals. *Circulation* 2000;101:E215–20. [PubMed: 10851218]
14. Barbieri R, Matten EC, Alabi AA, Brown EN. A point-process model of human heartbeat intervals: new definitions of heart rate and heart rate variability. *Am J Physiol Heart Circ Physiol* 2005;288:H424–35. [PubMed: 15374824]
15. Barbieri R, Brown EN. Analysis of heartbeat dynamics by point process adaptive filtering. *IEEE Trans Biomed Eng* 2006;53:4–12. [PubMed: 16402597]
16. Napadow V, Dhond R, Conti G, Makris N, Brown EN, Barbieri R. Brain correlates of autonomic modulation: combining heart rate variability with fMRI. *Neuroimage* 2008;42:169–77. [PubMed: 18524629]

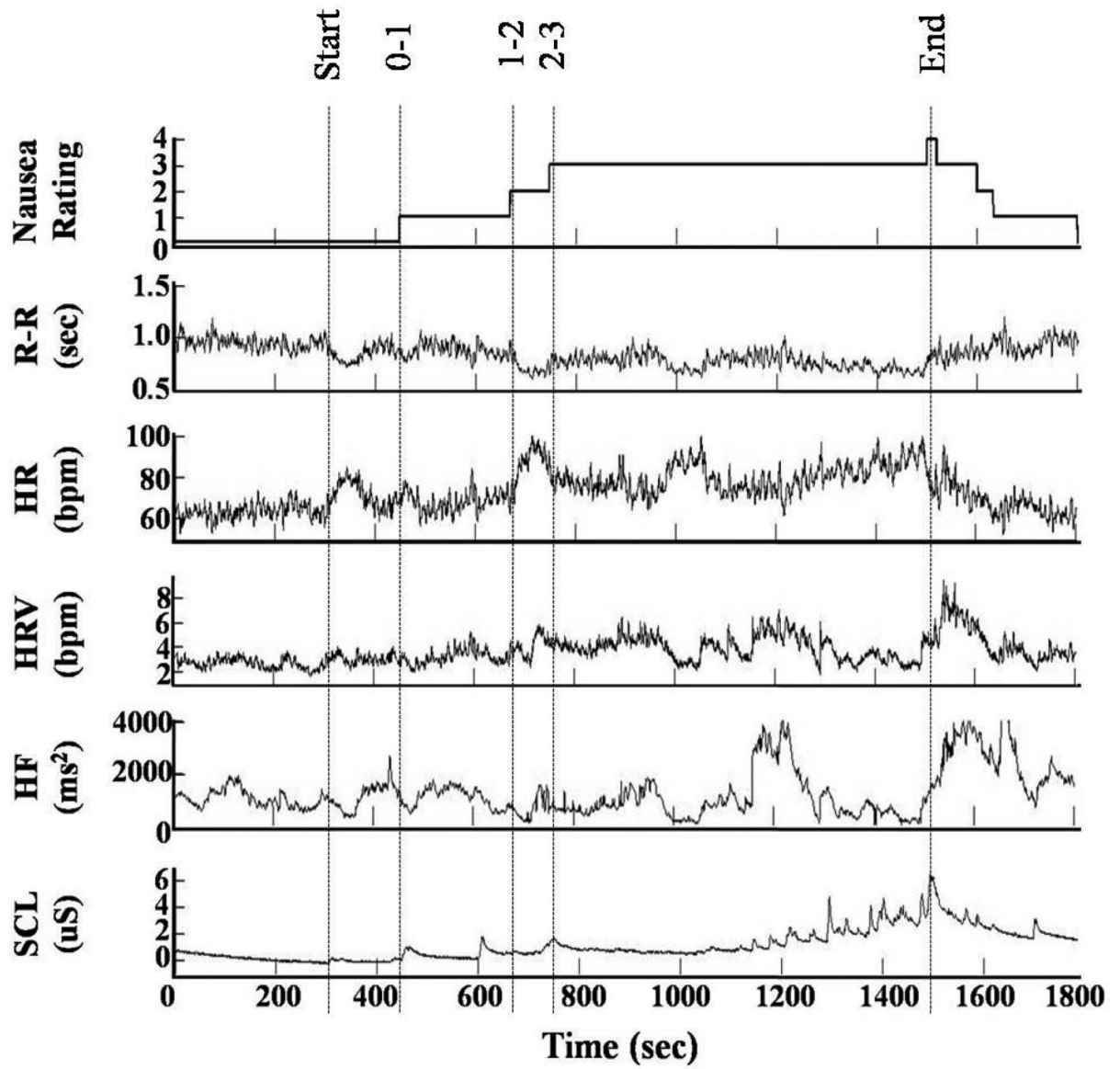


Figure 1. Data and instantaneous point process estimates from Subject 22: (A) Nausea level, (B) RR interval series, (C) instantaneous heart rate, (D) instantaneous HRV, (E) HF power, and (F) skin conductance level.

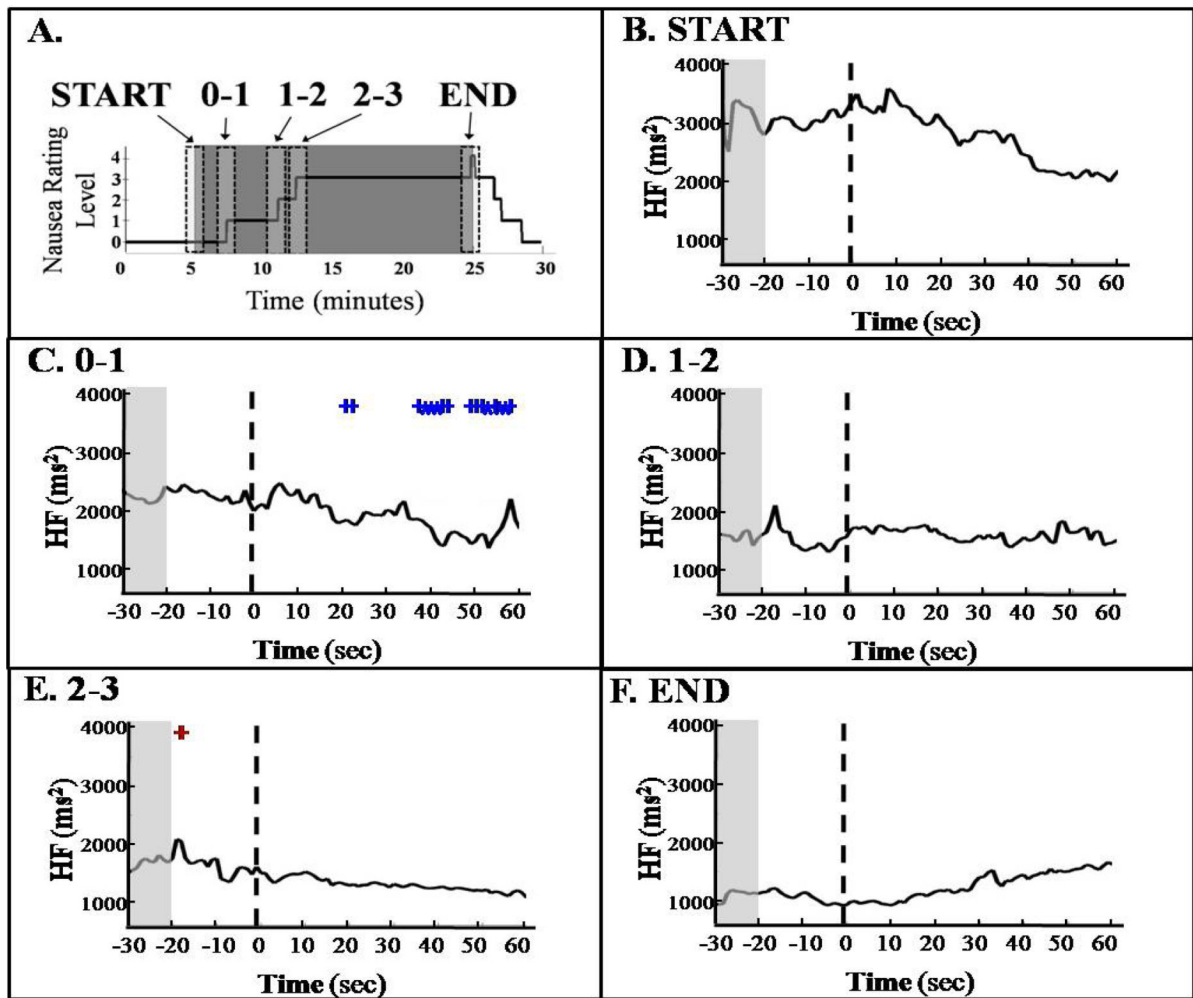


Figure 2.

HF Averaged Across Subjects. Each second of HF 20 s before an event to 60 s after an event was compared to the mean of the region between 30 s and 20 s before an event (paired t-test). Events included beginning (“START”) and end (“END”) of the stimulus as well as rating increases to “1” (“0-1”), “2” (“1-2”), and “3” (“2-3”). (+: $0.1 \geq p > 0.05$; *: $p \leq 0.05$)

Table 1

Average across subjects (mean \pm s.d.) of heart rate (HR), heart rate variability (HRV), high frequency power (HF), and skin conductance level (SCL) for selected regions of interest. Regions of interest include initial 5 min rest period (“Rest”) as well as periods at which subjects rated “1,” “2,” or “3.”

	Rest	“1”	“2”	“3”
HR (bpm)	73.7 \pm 13.0	79.5 \pm 13.6*	85.0 \pm 14.9*	86.4 \pm 17.6*
HRV (bpm)	3.8 \pm 1.3	4.0 \pm 1.5	4.0 \pm 1.2	3.9 \pm 1.0
HF (ms ²)	2409 \pm 4252	1831 \pm 3092	1642 \pm 3073 ⁺	1118 \pm 1610
SCL (uS)	2.6 \pm 4.9	3.7 \pm 5.4*	4.2 \pm 5.3*	4.8 \pm 5.8*

⁺ 0.1 \geq p>0.05

* p \leq 0.05; paired t-test with “Rest”